

# **Optimization of reversible electroporation for the destruction of an irregular brain tumor**

**BEE 4530 – Computer Aided Engineering – Applications to Biomedical Processes**

**Group 01**

**Taha Ahmad, Karann Putrevu, Remy Walk, Xuexiang Zhang**

# Table of Contents

<b>I. EXECUTIVE SUMMARY .....</b>	<b>3</b>
<b>II. INTRODUCTION TO ELECTROPORATION.....</b>	<b>5</b>
<b>III. PROBLEM STATEMENT AND DESIGN OBJECTIVES.....</b>	<b>6</b>
<b>IV. METHODOLOGY FOR MODELING TUMOR DESTRUCTION .....</b>	<b>7</b>
Schematic .....	7
<b>V. GOVERNING PHYSICS AND EQUATIONS.....</b>	<b>8</b>
<b>VI. RESULTS AND DISCUSSION .....</b>	<b>12</b>
Electric Potential and Field Distribution .....	12
Heat Transfer Model: Temperature Profile .....	12
Mass Transfer Model: Nanoporation and Concentration Profiles.....	13
Voltage and Diffusivity Sensitivity Analysis .....	15
Optimization and Design Recommendation.....	18
Validation.....	20
<b>VII. CONCLUSION AND FUTURE .....</b>	<b>23</b>
<b>VIII. APPENDIX A: MESH AND MESH CONVERGENCE .....</b>	<b>24</b>
<b>IX. APPENDIX B: REFERENCES .....</b>	<b>25</b>

## I. EXECUTIVE SUMMARY

The ability to localize treatments is of great relevance to many diseases, from cancer to blood clots. The drugs used for treatment are often cytotoxic or otherwise deleterious to healthy as well as diseased tissue, and simply flooding the body is not an option. Conversely, the physiochemical properties of these drug molecules can often prevent their penetration of the cell membrane in even the targeted area.

Reversible tissue electroporation serves as a method to bypass this barrier and introduce the drug into only targeted tissue. The instantaneous application of an electrical field (pulse) causes the transient formation of pores in the cell membrane that allow large molecules, including drugs, to pass into the cytosol. Such electroporation has found use clinically in electrochemotherapy, electrogenetherapy, and transdermal drug delivery.

However, the introduction of reversible electroporation into body tissue can have unintended consequences that require consideration. Sensitive areas of the body, such as the brain, may be subject to overheating if the applied voltage is too high, and the electrodes must be oriented so as to minimize the penetrance of drug into healthy tissue. In vivo experimentation on animal models has several limitations, including imperfect correlation to human application, small sample sizes, and prohibitive costs. Thus predictive models are required prior to human clinical trials to ensure that minimal collateral damage is done to surrounding tissue. For this study, a two-dimensional model was developed in order to maximize death within a brain tumor while minimizing death in the surrounding healthy tissue.

Given the complexity of the physics involved, the model was numerically implemented via the available software, COMSOL Multiphysics 4.3. A single pulse was applied to the domain and studied over five seconds. Pore distribution and pore size were linked to the strength of the electrical pulse implemented and the time post pulse. The reaction rate modeled the intake of drug (in this study, *bleomycin*) into the cell and was dependent on pore size, pore distribution, and local bleomycin concentration. Bleomycin was used for direct comparison with several other studies on electroporation that used the same agent.

Using this model, it was found that for the chosen irregular tumor, thermal stress was of minimal concern as it failed to kill any cells not already killed by bleomycin. The optimization of electrode orientation, distancing and voltage application yielded a horizontal orientation with 4.8 mm between the electrodes and an applied voltage of 275 Volts, which killed 91.28% of the tumor. The application of larger voltages killed more of the tumor, but relatively more healthy cells.

Sensitivity analysis on the voltage applied showed that the profile of electroporated cells followed the distribution of electric field lines, generally the  $1 \times 10^4$  V/m line. It follows that there is a great

deal of flexibility in the shape of the electroporated region that can be adjusted on a case-by-case basis.

The goal of this model was to provide an accurate and clinically relevant simulation of reversible electroporation for tumor destruction. This is the first model that optimizes a two-electrode approach to reversible electroporation with an irregular tumor model and surrounding healthy tissue, and thus provides clinicians with finer control and understanding of this methodology for application. However further refined models must still be completed for increased predictive power; such refinements include a three dimensional model, multiple pulses, and modeling of intracranial pressure changes.

## II. INTRODUCTION

The electrochemical and physical properties of the cell membrane limit the efficiency of molecular drugs requiring membrane penetration, including the antitumor antibiotic bleomycin. The effectiveness of molecular drugs requires introduction of the drug into targeted cells in the body; however, physiochemical parameters including molecular charge, molecular weight, and hydrophilicity, the chemical molecules are often unable to penetrate the cell membrane at a significant rate. Reversible electroporation creates temporary nanopores in the cell membrane by inducing an electric field in the tissue, thereby allowing normally impermeant molecules to enter cells. The precise mechanism of nanoporation is as yet unknown [1,2].

Electrical pulses are applied to the diseased tissue to create an electrical field from which nanoporation results and drug molecules diffuse into the cell; the pores remain open for a few seconds while the pulses are typically delivered on a time scale of microseconds [3,4,5,6]. Decay of pore number and pore size occurs exponentially after pulse application. Mathematical models are essential precursors to routine medical use for this invasive and potentially harmful procedure; they allow researchers to accurately predict, given a certain strength of pulse, the resulting size and number of pores as well as their time of persistence, in order to optimize the mass transfer of drugs into the tumor cells while minimizing damage to other surrounding healthy cells.

Significant prior research into the use of electroporation for cancer treatment has been either through clinical trials or mathematical models of generalized tumors modeled as spheres [4]. Newer research has expanded the breadth models such that they extend from the cellular level to the macroscopic level. These previous mathematical models have largely focused on malignant cells, neglecting the effects of electroporation on the surrounding healthy cells [3].

Especially when considering vital and sensitive organs such as the brain, these effects are of extreme clinical relevance. Electroporation runs the risk of both overheating due to the applied voltage and increased intracranial pressure due to the large amount of energy delivered to the brain. A 2013 study on the use of electroporation on rat brain tumors found that while rats that received treatment with bleomycin and electroporation survived an average of 3.1 days more than rats that received only electroporation, some rats died within three days of treatment due to edema and increased intracranial pressure [6].

The goal of this study was to create a mathematical model to predict the flux of drug molecules, specifically bleomycin, into a brain tumor while monitoring the death of healthy tissue due to either bleomycin or thermal stress. With this mathematical model, the optimal voltage, drug concentration and orientation of electrodes can be determined for clinical treatment.

### **III. PROBLEM STATEMENT AND DESIGN OBJECTIVES**

This study will develop and analyze computational mass transfer and heat transfer models to investigate drug delivery through reversible electroporation, which is the temporary permeabilization of the cell membrane using electrical fields.

This study will optimize electroporation in a model of the brain to maximize tumor destruction while minimizing healthy cell death using a normalized objective function. The parameters determining cell death are the local drug concentration and local temperature.

## IV. METHODOLOGY

Building off of previous single cell modeling work and a generalized macroscopic tumor space model, a two-dimensional domain containing an irregular brain tumor and healthy surrounding tissue was chosen as the subject of study [3,4]. Brain tissue was chosen for continuity with the work by Granot and Rubinsky from 2008, as well as to explore the deleterious effects on surrounding sensitive and important tissue [3].

Two-dimensional is not an optimal physical approximation of an irregular tumor with properties that differ from the surrounding tissue; however significant refinements and analysis of a two-dimensional model had to be completed before a three-dimensional model could be attempted. With this methodology, several different cross sections of the tumor and electrodes could be modeled and compiled into a three dimensional approximation. Moreover at the conclusion of the two-dimensional analysis implementation in a regular three-dimensional spherical tumor was attempted in COMSOL, which resulted in errors that the authors were unable to resolve in the available time period.

This model allows examination of heat transfer due to electrical field joule heating and mass diffusion due to pore formation on the membrane of individual cells. The heat transfer model provides information on temperature profile of the region, where 316.5 K is taken as the threshold for cell death due to thermal stress. The mass transfer model generates a concentration profile of the extracellular tissue concentration. When the bleomycin is taken up by cells the extracellular concentration drops according to the reaction rate. The threshold for cell death was determined to be a local drop in concentration from the initial condition of .005 mol/m<sup>3</sup> to .0049 mol/m<sup>3</sup>.

### Schematic

In reversible electroporation, the electrodes are inserted into or near the tumor tissue in brain. By taking a cross section of two inserted needle electrodes and an irregular tumor, a simplified 2-D domain of a tumor and its surrounding tissue was created (see Figure 1). The size of the surrounding rectangle of healthy tissue was validated in the results when there was neither mass nor heat flux at the boundaries for any of the voltages tested, and the assumption of electrical insulation was likewise borne out by the constant electrical field at the boundaries.

The tumor geometry came from an imaging paper [7]; the size (12 mm in diameter) was chosen because the model started with a basis of 2 electrodes 14 mm apart and it was initially desired that the tumor fit between the two electrodes; this size was simply maintained when it was decided that the electrodes should move inside the tumor.

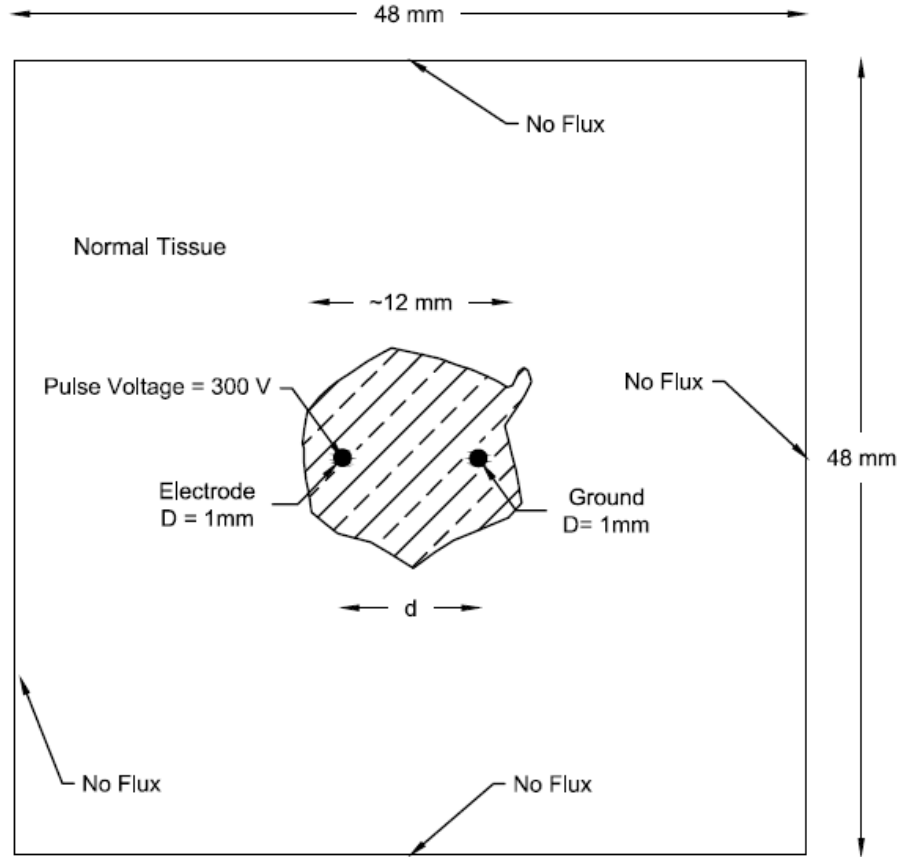


**Figure 1. Schematic drawing of two electrodes inserted in brain tissue.** At one electrode (solid circles), voltage is 300 V while the other is at 0 V (ground). There is neither heat flux nor mass flux at the outer boundaries and at the electrode boundaries. The initial concentration is 0.005 mol/m<sup>3</sup> at all regions. The outer boundaries are assumed to be insulating.

## V. GOVERNING EQUATIONS

Drug delivery of bleomycin into brain tissues using reversible electroporation technology is simplified and modeled in the COMSOL computational models using four physics modules: electrical current module, dilute species transport module, joule heating module and domain ordinary differential equation (DODE) module. The governing equations and their derivations come from Granot and Rubinsky's 2008 paper [3].

The governing equation for electrical field and potential is given as follow,

$$\nabla((\sigma + \varepsilon_0 \varepsilon) \nabla \varphi) = 0 \quad \text{[Equation 1]}$$

Here  $\varphi$  is the electrical potential,  $\sigma$  is the extracellular conductivity,  $\varepsilon_0$  is the vacuum permittivity and  $\varepsilon$  is the relative permittivity.

Heat generated at the electrodes over time are diffused through tissue, which is governed by the transient heat transfer equation:

$$\rho C_p \frac{\partial T}{\partial t} = \nabla(k\nabla T) + Q_m + \sigma(\nabla V)^2 \quad [\text{Equation 2}]$$

Here the two source terms refer to metabolic heat generation ( $Q_m$ ) and electrical joule heating ( $\sigma(\nabla V)^2$ ).

For mass transfer of bleomycin, the concentration of the drug in the extracellular space is governed by:

$$\frac{\partial c_{ex}}{\partial t} - \nabla(D\nabla c_{ex}) = R \quad [\text{Equation 3}]$$

Here  $c_{ex}$  is the concentration in extracellular space, D is the diffusivity coefficient and R is the reaction rate referring to cell uptake of drug (effectively removing it from the extracellular space and thus the domain).

Reaction rate can be calculated by:

$$R = JA_p/V_0 \quad [\text{Equation 4}]$$

$$J = -P \cdot (c_{ex} - c_{in}) \quad [\text{Equation 5}]$$

Here J is the mass flux per unit area and P is the permeability of the drug molecule through the membrane pores.  $V_0$  is the volume of a theoretical extracellular cube surrounding each cell.

The number of pores is described by the following differential equation:

$$\frac{dN_p}{dt} = \alpha e^{(V_m/V_{ep})^2} \left(1 - \frac{N_p}{N_0 e^{q(V_m/V_{ep})^2}}\right) \quad [\text{Equation 6}]$$

Here  $N_p$  is the number of pores on a single cell,  $\alpha$  is pore creation rate coefficient,  $V_m$  is the transmembrane voltage,  $V_{ep}$  is the characteristic voltage of electroporation,  $N_0$  is equilibrium pore density, and q is electroporation constant.

After solving the equation above, the area of all pores is calculated by assuming they are perfect-circle pores that decay exponentially after the pulse, described below:

$$A_p = \pi R_p^2 \cdot N_p N_p e^{-t/\tau} \quad [\text{Equation 7}]$$

$A_p$  is the total area of all pores on a single cell,  $R_p$  is the radius of pore, t is the time and  $\tau$  is the characteristic time of decaying. Without access to experimental pore measurements, radius is assumed to be constant across all pores.

The properties mentioned above in the governing equations are listed in Table 1.

**Table 1. Nomenclature and values used**

Symbol	Property	Value	Reference
$\epsilon_0$	Vacuum permittivity	$8.854 \times 10^{-12}$ F/m	3
$\epsilon_{\text{Brain}}$	Relative permittivity of brain	72	3
$\epsilon_{\text{Tumor}}$	Vitreous tumor permittivity	70	8
$\alpha$	Pore creation rate coefficient	$10^9$ m <sup>2</sup> s <sup>-1</sup>	3
$V_{\text{ep}}$	Characteristic voltage of electroporation	0.245V	3
$N_0$	Equilibrium pore density	$1.5 \times 10^9$ m <sup>-2</sup>	3
$q$	Electroporation constant	2.46	3
$\rho$	Brain density	1050 kg/m <sup>3</sup>	8, 9
$k$	Brain conductivity	0.51W/mK	10
$C_p$	Brain	3630 J/kgK	11
$T_i$	Initial brain temperature	36.85°C (= 310K)	12
$P_{\text{Brain}}$	Brain permeability	$9.8 \times 10^{-7}$ m/s	13
$P_{\text{Tumor}}$	Brain tumor permeability	$6.86 \times 10^{-7}$ m/s	13, 14
$\sigma_{\text{Brain}}$	Electrical conductivity of brain	0.88236 S/m	15
$\sigma_{\text{Tumor}}$	Electrical conductivity of tumor	1.4706 S/m	15
$V_0$	Volume of extracellular space per cell	$1 \times 10^{-12}$ m <sup>3</sup>	3
$D$	Diffusivity	$1 \times 10^{-10}$ m <sup>2</sup> /s	3

The thresholds for cell damage are given in Table 2. The temperature for cell death was taken directly from a 2010 textbook [16]. The threshold for cell death was found using the following equation derived from Granot and Rubinsky's 2008 work [3]:

$$C_{\text{crit}} = C_0 - \left( \frac{N}{N_A V_0} \right) \quad \text{[Equation 8]}$$

Here  $N_A$  is Avogadro's number and  $N$  is the number of molecules entering the cell.  $N=2000$  molecules will induce 100% cell mortality [17]. This would yield a  $C_{\text{crit}}$  of .004999996679 mol/m<sup>3</sup>. However, when applied to the model, this overestimates cell death in healthy regions because the bleomycin will diffuse from the healthy regions to the electroporation region, reducing local concentrations such that they appear dead. Since the results gave clearly defined areas of electroporation and since .0049 mol/m<sup>3</sup> consistently outlined this area, this was the threshold chosen. All areas below this threshold are assumed dead, and all areas above this are assumed alive.

**Table 2. Threshold levels for cell death**

Symbol	Description	Threshold Level
$C_{\text{crit}}$	Extracellular drug concentration for cell death	0.0049 mol/m <sup>3</sup>
$T_{\text{crit}}$	Temperature for hyperthermic cell death	43 °C (316.15K)

## Pulsing Function

As per reversible electroporation protocol, the voltage was not held constant during the simulation. For the simulation, the voltage was held at a maximum for 0.1 seconds and dropped to zero volts immediately afterwards as seen in Figure 2. A single pulse was used in the simulation.

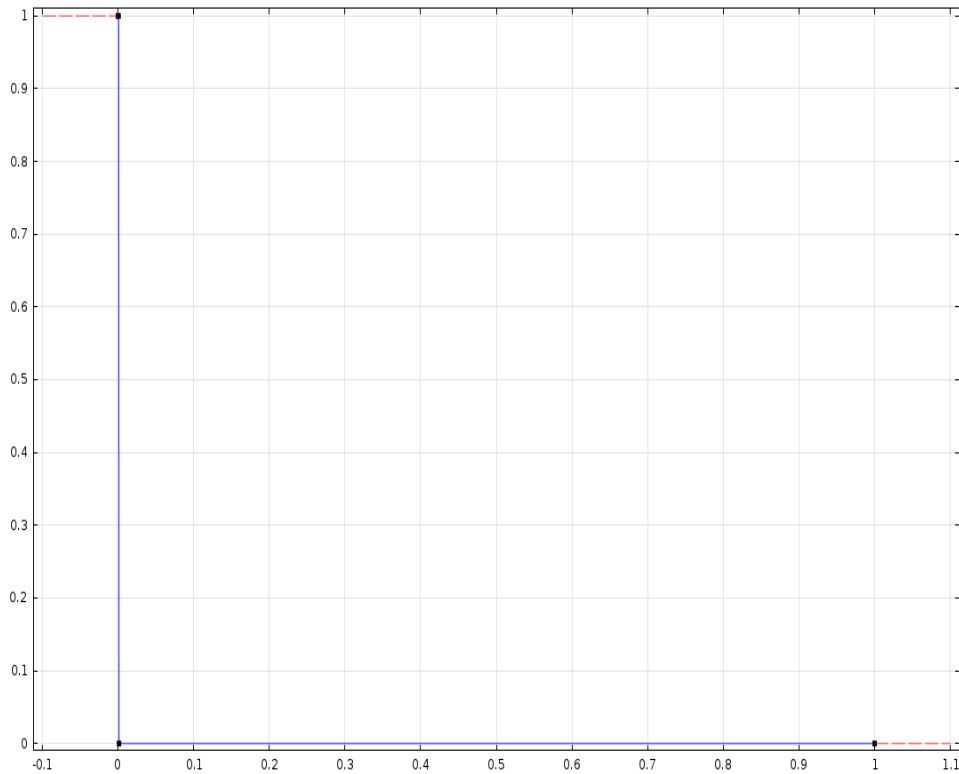


**Figure 2. Voltage pulsing function.** The voltage was multiplied by this function to implement a pulsing voltage.

## VI. RESULTS AND DISCUSSION

Implementation of the governing equations and the boundary conditions was done in COMSOL Multiphysics 4.3 with the electrical current, joule heating, dilute species transport and domain ODE modules over a five second time period.

### Electric Field Profile:

The electric potential (V/m) profile depended on the voltage applied and the distance between the electrodes. The maximum potential occurred around the electrodes and decreased radially outward. The resulting electrical field potential profile is largely symmetric about the y- axis as seen in Figure 3. Irregularities close to the tumor boundary are due to differing electrical properties of the tumor and the healthy tissue (see Table 1)

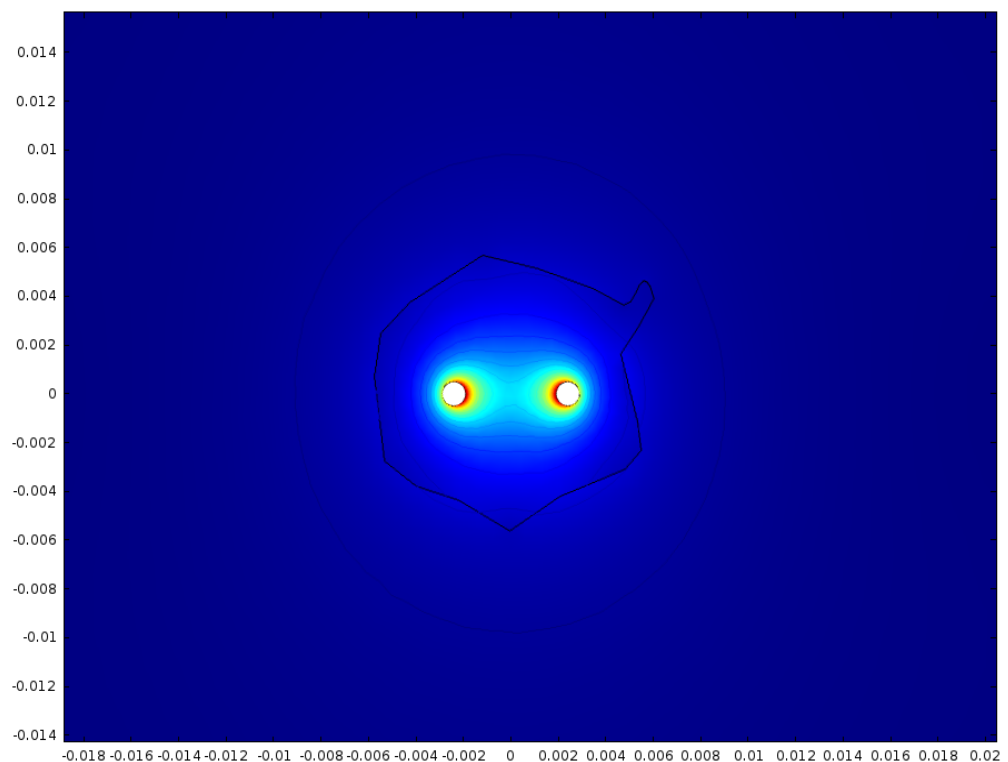


**Figure 3. Electric potential profile with contours:** Electric potential (V/m) profile with an applied voltage of 275 V and 4.8 mm between the electrodes. Irregularities at tumor edges are due to differential electrical properties of the tumor and the surrounding tissue.

### Heat Transfer in Tissue:

A consequence of applying a voltage to the brain is a rise in temperature due to joule heating. To test whether not a short pulse of high voltage would cause cell death, a voltage of 1000 V (above the voltage range of interest) was applied with the 9.6 mm between the electrodes, the maximum distance of interest (maximum because largest distance tested that keeps electrodes within the tumor). The resulting temperature profile shows minimal heating in the surround healthy brain cells

as seen in Figure 4. While the temperature localized to the electrodes does exceed the 316.15 K threshold for cell death, this region is significantly smaller than and wholly within the region affected by bleomycin (see Figure 7 d) for an example of the region affected by bleomycin after a 1000 V pulse). Thus, deleterious effects of heating can be ignored for electroporation with voltage less than 1000 V.

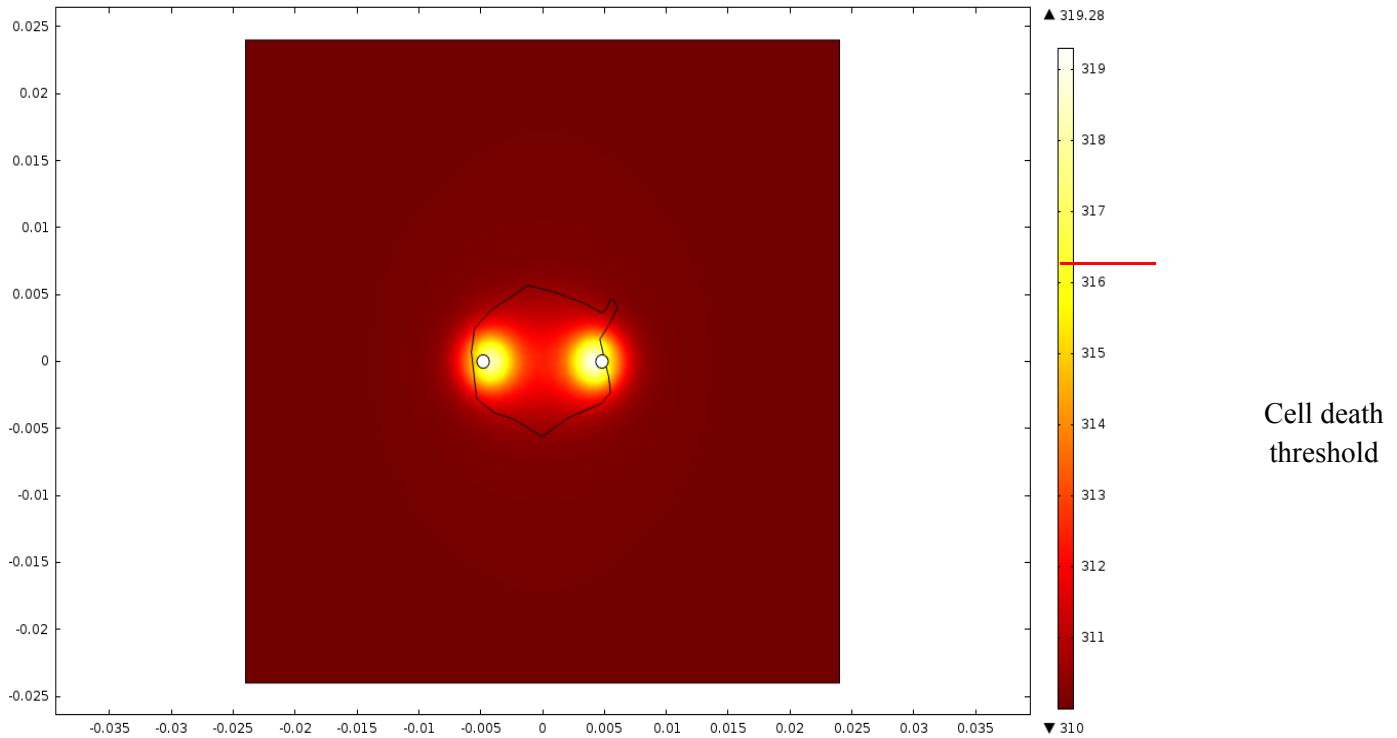


**Figure 4. Temperature profile at 1000 V after five seconds.** The temperature profile follows the shape of the electric potential with maximum temperature change within the tumor region. Red line on scale indicates approximate cell death threshold.

### Mass Diffusion of Bleomycin in Brain Tissue:

The applied voltage creates pores in the tumor and brain tissues, which allows the bleomycin to enter the cells. Initially, the extracellular space of the tissue is flooded with a concentration of  $0.005 \text{ mol/m}^3$ . The decreasing concentration indicates the bleomycin leaving the extracellular space and entering a cell. The simulation ran for five seconds as this was when the minimum domain concentrations within the electroporated regions occurred (initially, it was run up to 10 seconds and concentration profiles at each second were evaluated), indicating maximum uptake of bleomycin. Afterwards, diffusion of bleomycin from the non-electroporated regions has a greater effect than the reaction term within Equation 3. Figure 5 shows the concentration profile at 0, 1 and 5 seconds. The electroporated region is characterized by a sharp gradient. Generally the electroporated region itself has a sharply defined ring towards the edge. It should be noted that due to the greater permeability of healthy tissue, a continuously electroporated region that spans the tumor-healthy interface has a lower local bleomycin concentration (more cell uptake of bleomycin) on the healthy side.

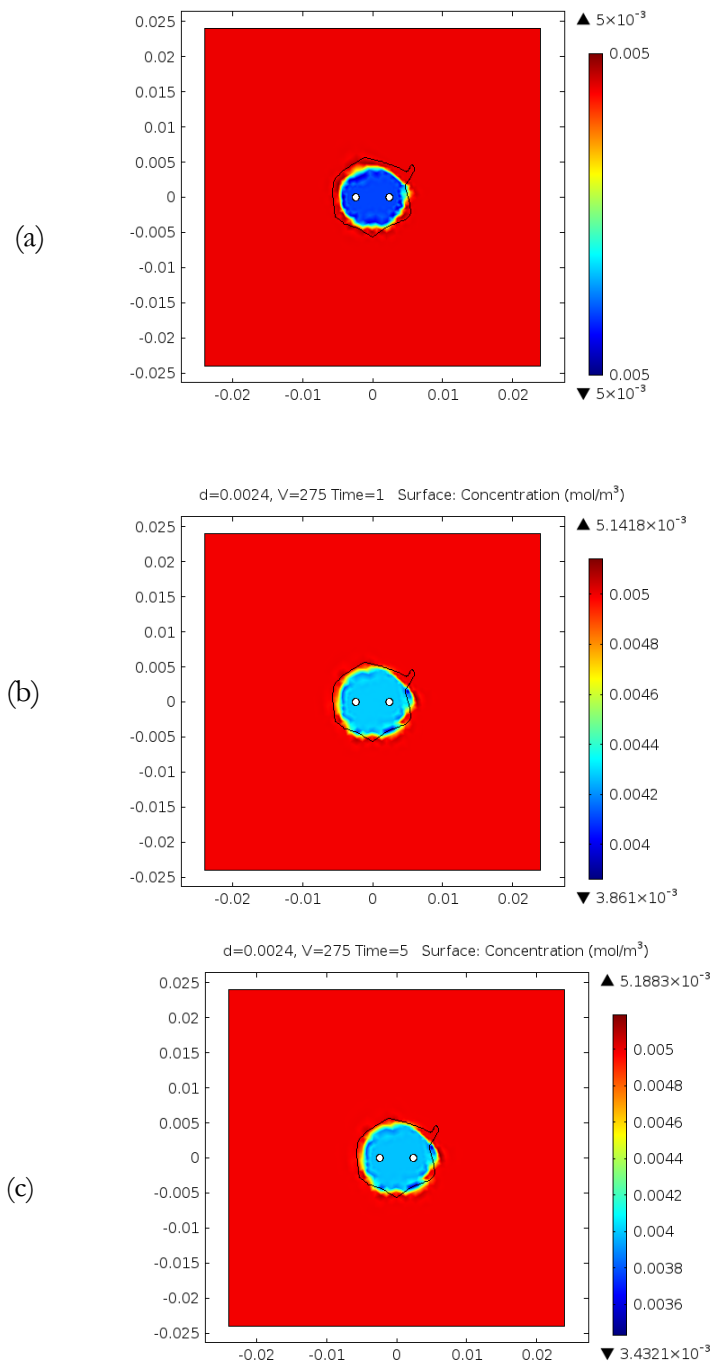


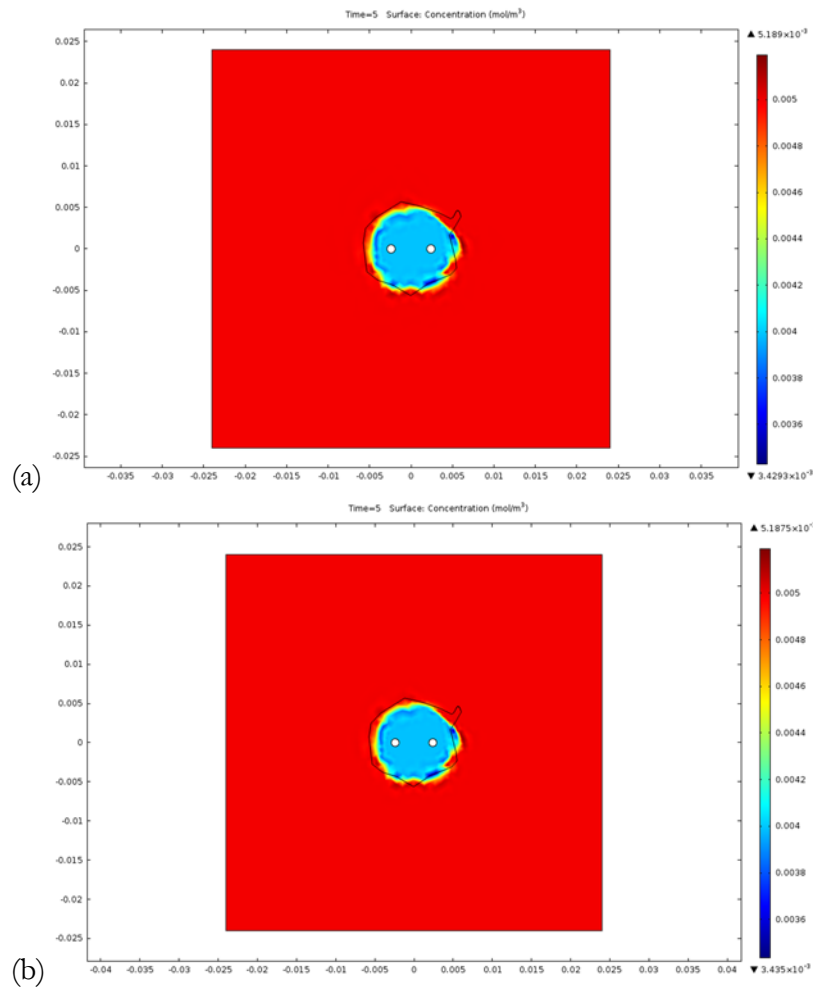
**Figure 5. Concentration profile over time.** Concentration profiles at (a)  $t = 0$  s (b) at  $t=1$ s and (c) at  $t=5$ s. Boundary conditions are no flux at rectangle edges and initial condition of  $0.005 \text{ mol/m}^3$  everywhere. Although the profile remains similar between time steps, the concentration is decreasing. Note that  $d$  in the plot title refers to half the distance between the electrodes; everywhere else  $d$  is the entire distance between electrodes unless otherwise noted.

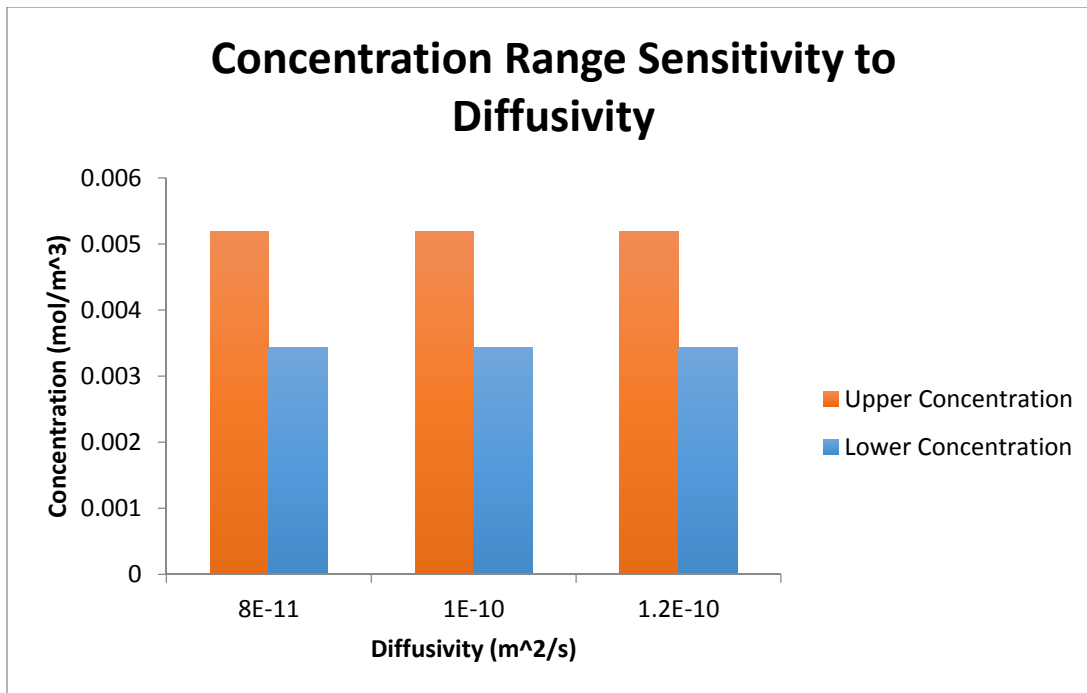
### Sensitivity Analysis:

Prior to optimization sensitivity analyses were run on the variable input voltage, as well as on diffusivity, as diffusivity was the parameter with the highest degree of uncertainty; Granot and Rubinsky explicitly characterize the assumed diffusivity value as a ‘reasonable’ approximation [3].

#### 1. Diffusivity

A sensitivity analysis was performed on the value of the diffusivity to determine the sensitivity of the concentration profiles to diffusivity coefficients 20% below and above the base value of  $1.0 \times 10^{-10} \text{ m}^2/\text{s}$ . As seen in Figure 6, neither the qualitative concentration profiles nor the concentration bounds change appreciably with a change in diffusivity.





(c)

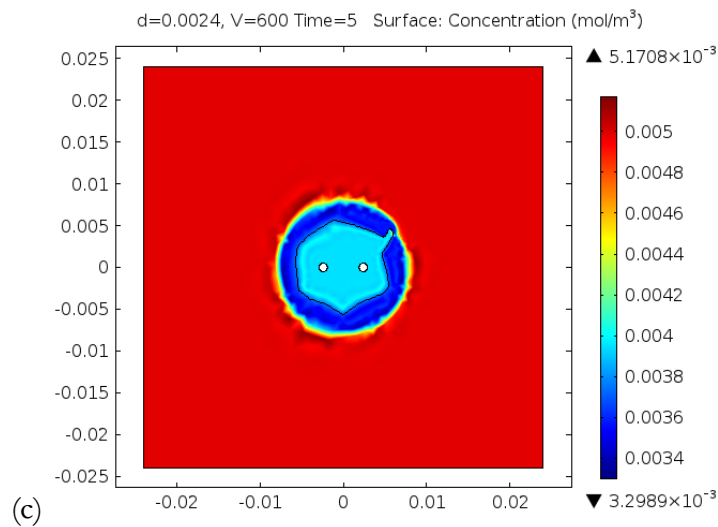
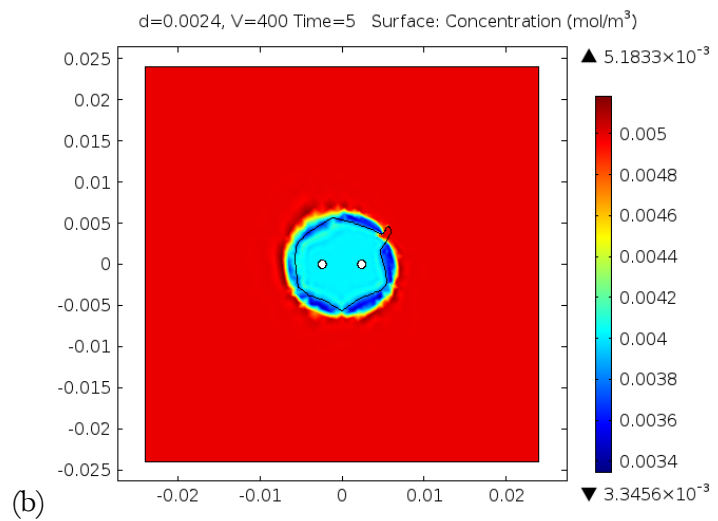
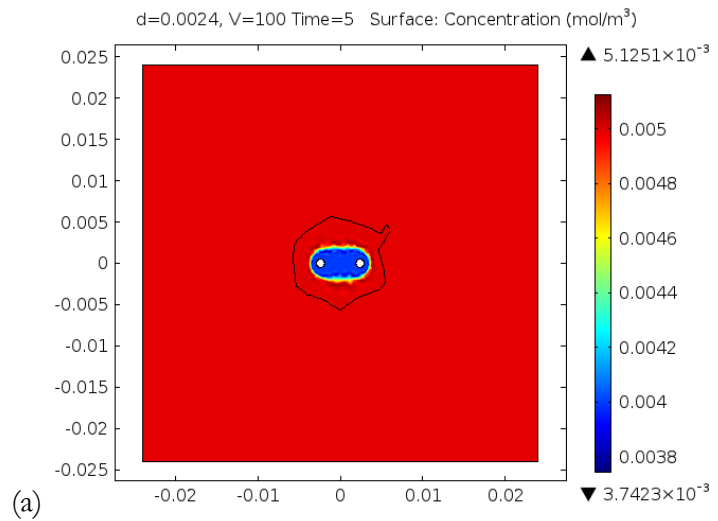
**Figure 6. Sensitivity Analysis for Diffusivity.** Profiles with diffusivity equal to (a)  $0.8 \times 10^{-10} \text{ m}^2/\text{s}$  and (b)  $1.2 \times 10^{-10} \text{ m}^2/\text{s}$ . Voltage is 275 V, and distance between electrodes is 4.8 mm. Also shown is a bar graph (c) of upper and lower concentration for each diffusivity value.

The insignificant change in the concentration profile with change in diffusivity signifies that on the short time scale simulated, the delivery of bleomycin into the cells is not limited by the diffusion of drugs through extracellular space. The limiting factor on a 5 second time scale, therefore, is the reaction rate process of drug crossing the cell membrane. This conclusion is valid only on the time scale of 5 seconds since beyond 5 seconds has not been analyzed in this simulation. Physics may evolve differently with longer time scales, especially as it has been previously noted that the relative influence of diffusivity on the concentration profile increases past five seconds.

## 2. Voltage

The voltage applied is a parameter controlled completely by the doctor using reversible electroporation; the voltage is an important factor that determines the concentration profile. Sensitivity analysis of the voltage helped narrow down a voltage range in which a meaningful percentage of tumor cells reached the critical concentration while minimizing healthy brain cell death. The voltages applied were 100, 400, and 1000 V. The shapes of the electroporated areas characteristically followed electric field lines; specifically, the electroporated region is generally in the same region defined by the contour  $1 \times 10^4 \text{ V/m}$ . It should be noted that due to the greater permeability of healthy tissue, a continuously electroporated region that spans the tumor-healthy interface has a lower local bleomycin concentration (more cell uptake of bleomycin) on the healthy side.

Based off of this sensitivity analysis, starting voltages for optimization were chosen to fit the shape of the tumor. Given the fairly circular appearance of the irregular tumor in this experiment, voltages around 400 V were used to begin.



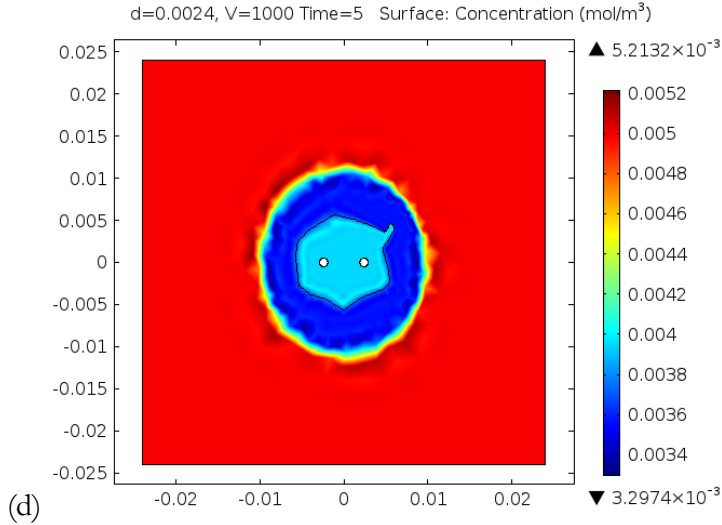


**Figure 7. Example concentration profiles at various voltages.** The concentration profiles at (a) 100 V, (b) 400 V, (c) 600 V and (d) 1000 V. The permeability of the tumor tissue is 30% less than that of brain tissue resulting in the abrupt change in concentration at the brain/tumor boundary. Note that ‘d’ in the plot title refers to half the distance between the electrodes; everywhere else ‘d’ is the entire distance between electrodes unless otherwise noted.

### Optimization:

An optimal scenario for the model would be 100% tumor cell death and no healthy cells killed. Cell death was indicated by area in each domain with concentration below  $0.0049 \text{ mol/m}^3$  (Table 2). In the objective function (J), the weight of killing a tumor cells is equal to the weight of killing a healthy brain cell as seen in Equation 9. For optimization of the model, the objective function must be maximized thereby killing mostly tumor cells while minimizing damage to the brain. The function is divided by the total number of tumor cells in order to normalize the function; at 100% tumor death and no healthy cell death the function is equal to 1.

$$J = \frac{\sum \text{Dead Tumor Cells} - \sum \text{Dead Healthy Cells}}{\sum \text{Total Tumor Cells}} \quad [\text{Equation 10}]$$

The voltage, electrode orientation and the distance between the electrodes were varied to obtain an optimal configuration. As there are theoretically infinite combinations that could be tested, parameters were limited as follows for simplification: the electrodes were constrained to the x and y-axes; distances were confined to 4.8, 7.2, and 9.6 mm apart; the voltages ranged from 100 V to 500 V with the smallest increment tested at 25 V.

#### 1. Vertical orientation of Electrodes

The first configuration tested was with the electrodes on the y-axis. A parametric sweep varied simultaneously the voltage and the distance between the electrodes resulting in an optimal configuration of 400 V at distance of 7.2 mm between the electrodes as seen in Figure 8 below. In this configuration, 86.9% of tumor cells were killed.

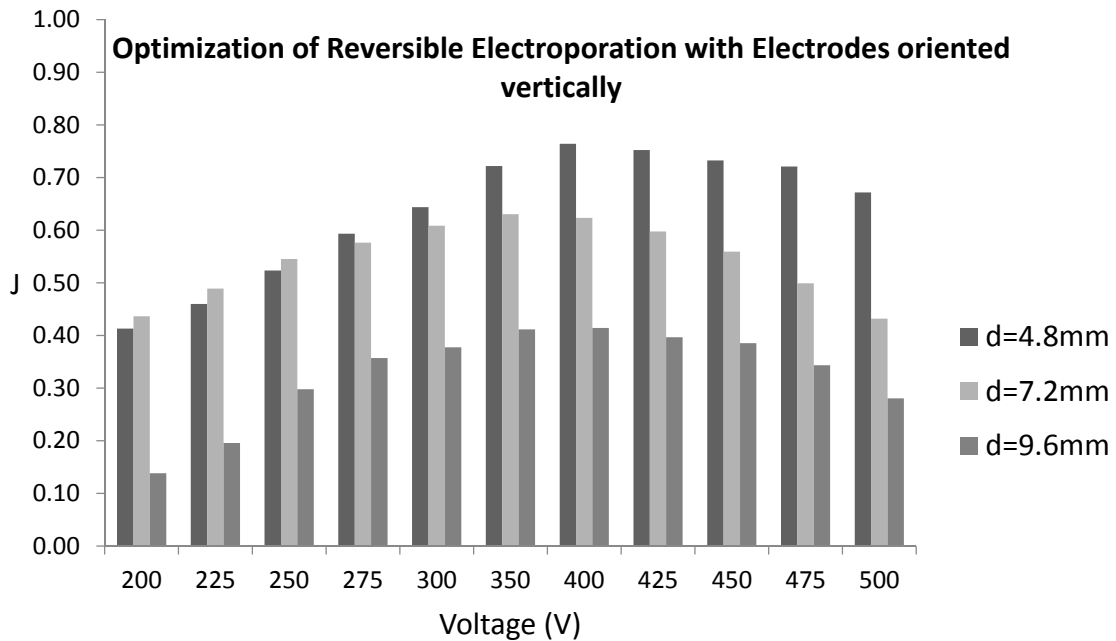


**Figure 8. Vertical Optimization.** The objective function versus voltage was plotted at the three distances investigated with the electrodes on the y-axis. The objective function reaches a max at 0.76, which is associated with an 86.9% tumor cell death.

## 2. Horizontal orientation of electrodes

The second configuration constrained the electrodes to the x-axis. As in the vertical optimization, a parametric sweep varied the voltage and distance between the electrodes. The optimal configuration with the electrodes on the x-axis occurred at 275 V with 4.8 mm between the electrodes as seen in Figure 9. This configuration is associated with a 91.28% cell death. The design recommendation would thus be to implement this set of parameters.

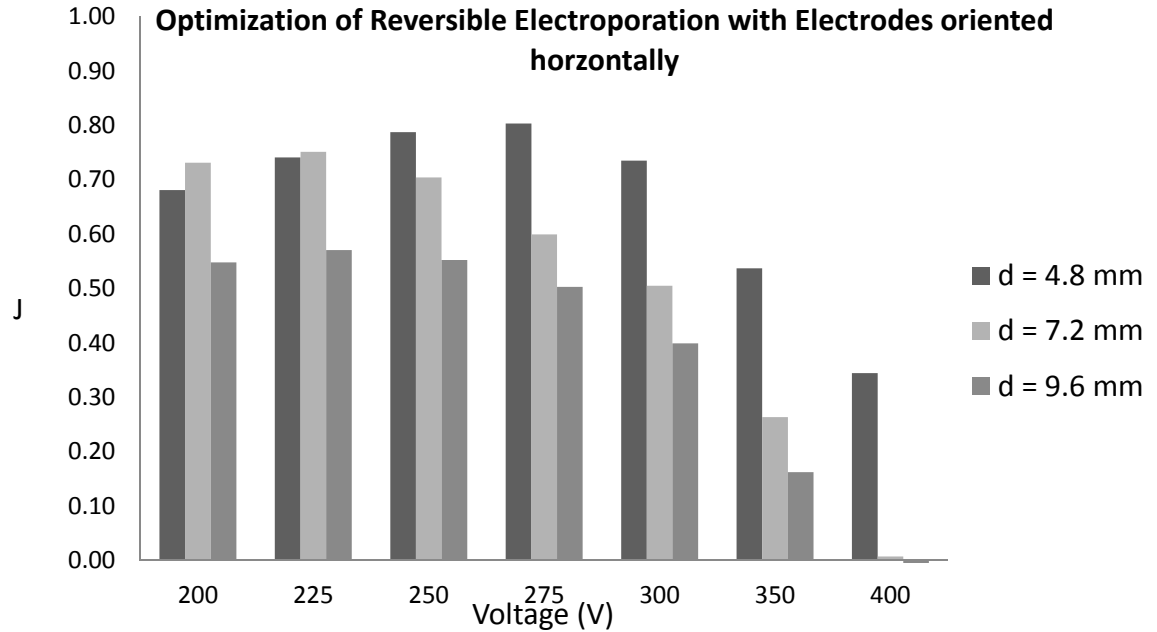
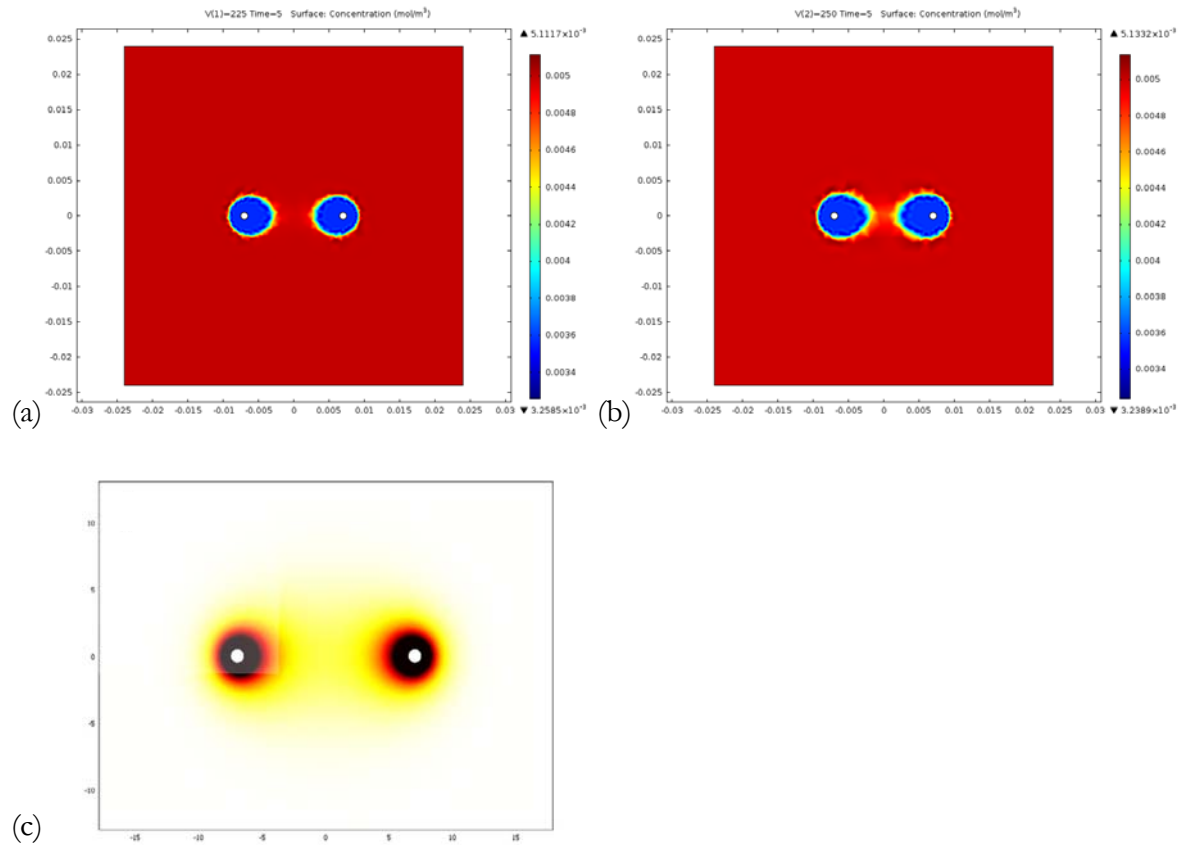


**Figure 9. Horizontal Optimization.** The objective function versus voltage was plotted at the three distances investigated with the electrodes on the x-axis. The objective function reaches a max at 0.80, which is associated with a 91.28% tumor cell death.

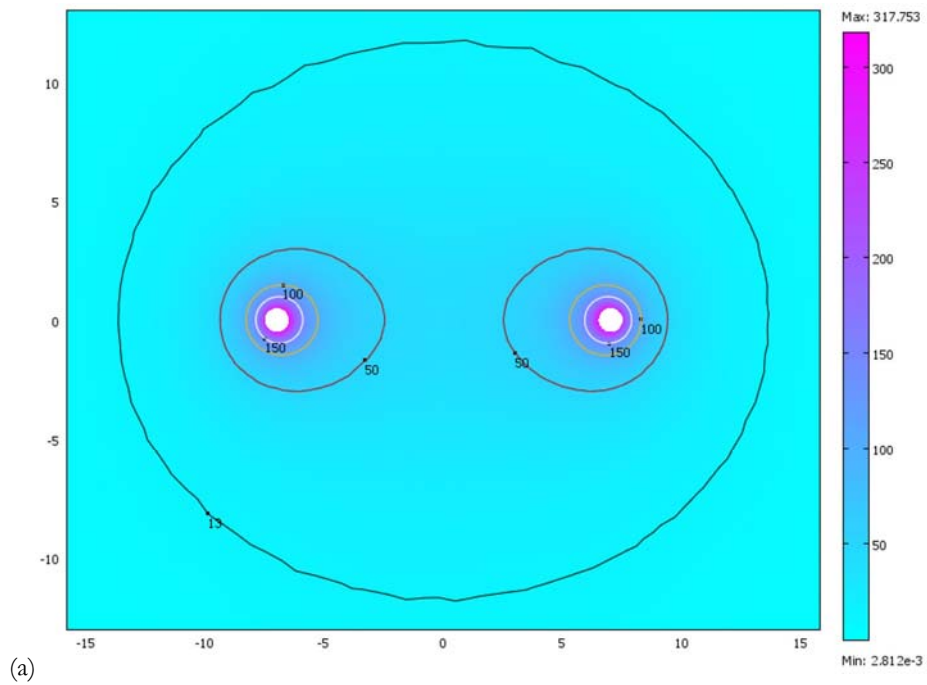
### Validation

To validate the results of the model, the model was modified to match a 2008 model (Granot et. al., 2008) from which the governing equations were pulled. The simulation was running using the same configuration as in the 2008 paper. The same trend wherein the electroporated region followed electric field distributions was observed; however, at the 1000 V used in the paper the particular concentration profiles did not match. Varying the way functions were input into the model and modifying assumptions about the model's boundary and initial conditions did not alter the results. Efforts were made to reach out to both the authors of the 2008 paper, but no useful feedback was obtained. Given that the paper's implementation was vague and that scales on the figures were generally missing, the conclusion was reached that 2008 paper likely had some sort of numerical error in its results. Decreasing the voltage to between 225 and 250 V yielded very similar concentration profiles to the one given by the paper at 1000 V (Figure 10) [3].

Finally, it should be noted that the distribution and magnitude of electric fields at 1000 V is not substantially different from the distribution obtained by the paper (Figure 11). Thus it follows that the error in the 2008 paper likely lies somewhere in the implementation of either the term for pore formation or the term for reaction rate [3].



**Figure 10. Validation of concentration profiles.** The concentration profiles of (a) 225 V, 5s (b) 250 V, 5s (c) Granot, et al. 2008 model 1000 V, 5s. Granot et al. shows no scale for concentrations [3].



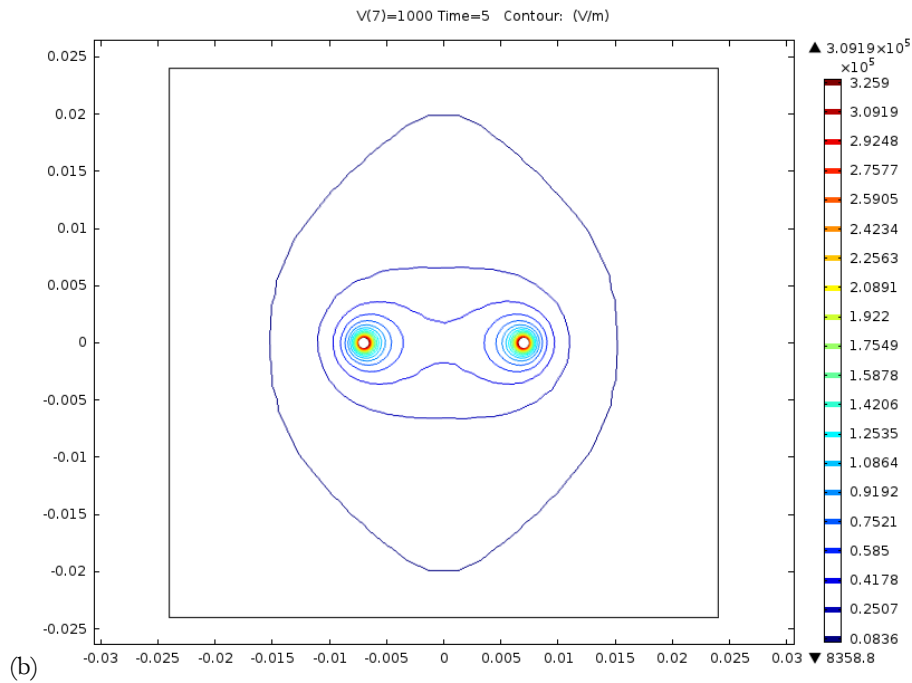


**Figure 11. Validation of Electric Field Distributions.** The electric field distributions for (a) Granot and Rubinsky (2008) at 1000 V [lines in kV/m] [3] (b) 1000 V [lines in V/m]. Magnitudes and range match up.

## VII. CONCLUSION AND FUTURE

### Conclusion

The model returned sensible results for the concentration profile. The applied voltage led to bleomycin uptake in the tumor region, creating a concentration profile with a strong resemblance to the profile created for pore formation. Both pore formation and concentration profiles follow the contours of the electric field, generally following the field line for  $1 \times 10^4$  V/m. Validation corroborates this trend, though no models or experimental results are available for validation of precise numerical answers.

Interestingly, reversible electroporation as applied in this model shows very highly localized action, with sharp gradients between affected and unaffected regions. This is likely because the pores must be of a minimum size for the drug to enter, setting up a threshold. The exponential decay of pore size and pore number also likely exacerbate this sharp gradient. Along with the flexibility in shape and size the affected regions, this localization makes the method highly desirable for sensitive tissue treatment. At the voltages tested and at optimal orientations along the horizontal axis in particular, over 90% tumor destruction was achieved with minimal healthy cell destruction with just two electrodes. Varying the electrode orientation, distancing, and voltage in more and smaller increments can likely increase this efficiency and increasing the number of electrodes would give finer control to the clinician. In addition, the heating effect of the electrodes at the highest tested voltage did minimal damage to healthy cells; most damage was contained in the tumor itself, and no damage from heating was collateral to that done by the action of bleomycin itself. Thus, the model provides further evidence of the utility of this two-pronged approach in combating brain cancer.

### Future

For a complete model of reversible electroporation a three-dimensional model is necessary given that: tumors are irregular in three dimensions as well as two; tumors have different electrical, thermal, and diffusive properties from healthy tissue. As noted, this was attempted but in the short time available the errors that COMSOL returned were not readily absolved. In addition, future model research should involve the implementation of multiple voltage pulses to better simulate clinical implementation. The limitations of COMSOL in implementing modular time alongside the pore equation prevented such a pulse from being properly used in this model; however, a model with such voltage pulses would more accurately represent clinical conditions. It is possible that a different numerical solver than those provided by COMSOL will be necessary. Finally, one in vivo experiment on rats found rats dying from increased intracranial pressure; measuring this would be of great benefit to optimization and thus clinical safety [7].

## VIII. APPENDIX A: MESH AND MESH CONVERGENCE

### Mesh Analysis

To further validate the accuracy of the model's results, mesh convergence was performed to ensure that special discretization error was not significant. The mesh used was free triangular with higher density around the electrodes. The mesh converged at 3599 elements as seen in Figure 12. Figure 13 shows the mesh, with more elements in areas of steep gradients.

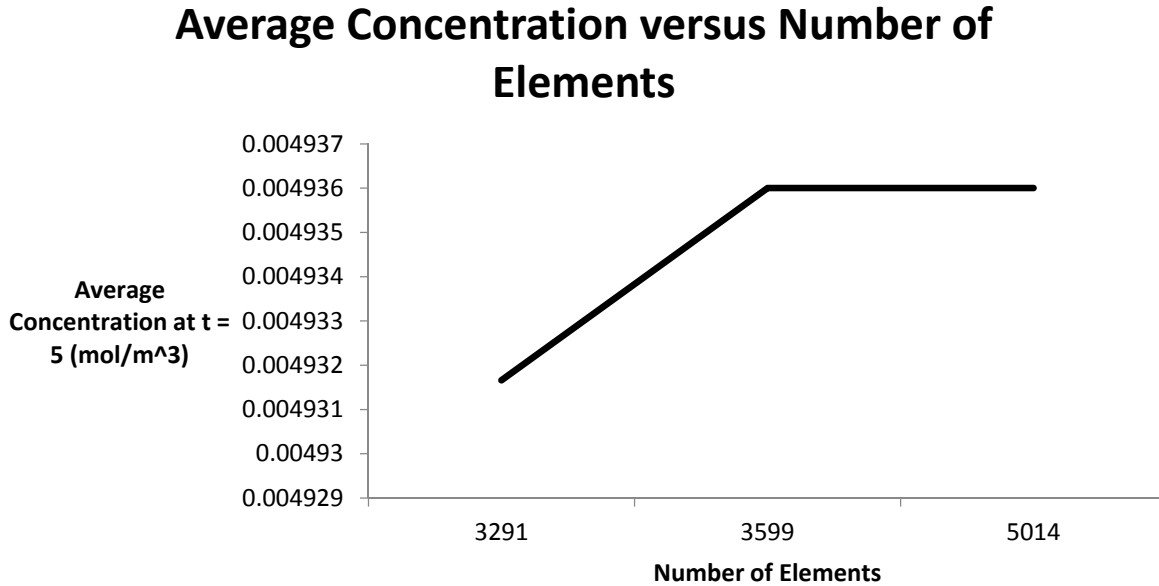


**Figure 12. Mesh convergence for average Concentration.** The mesh converged at 3599 with relation to the final average concentration of bleomycin.

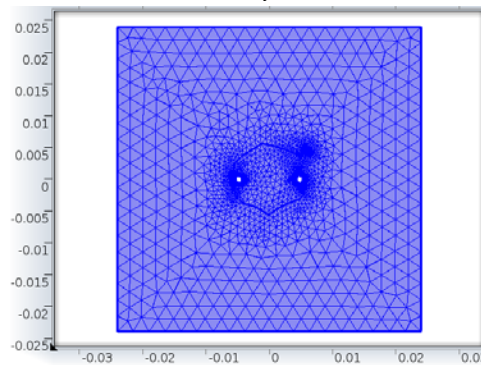


**Figure 13. Mesh for the tumor and normal tissues.** Triangular meshes are implemented in the model. More elements are at the boundary of tumor and normal tissue, as well as around the two electrodes.

## IX. APPENDIX B: REFERENCES

- [1] Linnert, M., & Gehl, J. Bleomycin treatment of brain tumors: An evaluation. *Anti-Cancer Drugs*, 157-164, 2009.
- [2] Agerholm-Larsen, B., Iversen, H., Ibsen, P., Moller, J., Mahmood, F., Jensen, K., & Gehl, J. (2011). Preclinical Validation of Electrochemotherapy as an Effective Treatment for Brain Tumors. *CANCER RESEARCH*, 3753-3762.
- [3] Y. Granot and B. Rubinsky, 'Mass transfer model for drug delivery in tissue cells with reversible electroporation', *International Journal of Heat and Mass Transfer*, vol. 51, no. 23-24, pp. 5610-5616, 2008.
- [4] W. Krassowska and P. Filev, 'Modeling Electroporation in a Single Cell', *Biophysical Journal*, vol. 92, no. 2, pp. 404-417, 2007.
- [5] Jordan, C.A., Neumann, E., Sowers, A.E. (2013). Electroporation and Electrofusion in Cell Biology. *Springer Science and Business Media*, 104.
- [6] Chenping Yu, Guilherme C. S. Ruppert, Dan T. D. Nguyen, Alexandre X. Falcao, and Yanxi Liu. Statistical Asymmetry-based Brain Tumor Segmentation from 3D MR Images, *5th international joint conference on biomedical engineering systems and technologies*, 2012.
- [7] Ljungvall M., Salford, L. G., and Persson, B. R. R., (2013). Treatment of brain tumours with electroporation and bleomycin in an in vivo rat model. (Master Thesis Med. Magnus Ljungvall, autum 2000; sem.11), *Acta Scientiarum Lundensia*, Vol. 2013-001, pp 1-10, ISSN 1651-5013
- [8] Duck, F. (2013) *Physical Properties of Tissues: A Comprehensive Reference Book*. *Academic Press*,
- [9] J. Buzby (2003, June 10) Available: <http://en.allexperts.com/q/Molecular-Biology-1353/density-brain.htm>
- [10] Barber, T., Brockway, J., Higgins, L. (1970). The Density of Tissues in and about the Head. *Acta Neurologica Scandinavica*, 1600-5606.
- [11] Hasgall PA, Di Gennaro F, Baumgartner C, Neufeld E, Gosselin MC, Payne D, Klingenberg A, Kuster N, "IT'IS Database for thermal and electromagnetic parameters of biological tissues," Version 2.6, January 13th, 2015. [www.itis.ethz.ch/database](http://www.itis.ethz.ch/database)
- [12] Busto, R., Dietrich, Globus, Ginsberg. (1989) The importance of brain temperature in cerebral ischemic injury. *Stroke*, 1113-1114

[13] Greenberg, H., Chandler, W., Sandler, H. (1999) Brain Tumors. *Oxford University Press*

[14] Baronzio GF, Gramaglia A, Baronzio A, et al. Influence of Tumor Microenvironment on Thermoresponse: Biologic and Clinical Implications. In: Madame Curie Bioscience Database [Internet]. Austin (TX): Landes Bioscience; 2000-. Available from: <http://www.ncbi.nlm.nih.gov/books/NBK6245/>

[15] Garcia, P., Rossmeisl, J., Davalos, R. (2011) Electrical Conductivity changes during irreversible electroporation treatment of brain cancer. *Conference Proceedings IEEE Engineering in Medicine and Biology Society*. 739-742

[16] A. Datta and V. Rakesh, *An introduction to modeling of transport processes*. Cambridge, UK: Cambridge University Press, 2010.

[17] Poddevin B, Orłowski S, Belehradek J, Mir LM. Very high cytotoxicity of bleomycin introduced into the cytosol of cells in culture. *Biochemical Pharmacology* 1991;42:S67–S75. [PubMed: 1722669]